analytical chemistry

pubs.acs.org/ac Article

Leveraging the HMBC to Facilitate Metabolite Identification

Fatema Bhinderwala, Thao Vu, Thomas G. Smith, Julian Kosacki, Darrell D. Marshall, Yuhang Xu, Martha Morton, and Robert Powers*

Cite This: *Anal. Chem.* 2022, 94, 16308−16318 Read Online

ACCESS | Metrics & More | Article Recommendations | Supporting Information

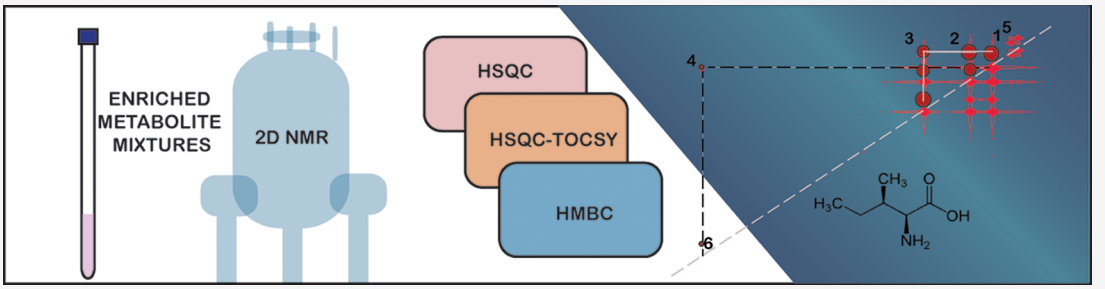

ABSTRACT: The accuracy and ease of metabolite assignments from a complex mixture are expected to be facilitated by employing a multispectral approach. The two-dimensional (2D) $^{1}H-^{13}C$ heteronuclear single quantum coherence (HSQC) and 2D $^{1}H-^{1}H$ total correlation spectroscopy (TOCSY) are the experiments commonly used for metabolite assignments. The 2D $^{1}H-^{13}C$ HSQC−TOCSY and 2D $^{1}H-^{13}C$ heteronuclear multiple-bond correlation (HMBC) are routinely used by natural products chemists but have seen minimal usage in metabolomics despite the unique information, the nearly complete $^{1}H-^{1}H$ and $^{1}H-^{13}C$ and spin systems provided by these experiments that may improve the accuracy and reliability of metabolite assignments. The use of a ^{13}C-labeled feedstock such as glucose is a routine practice in metabolomics to improve sensitivity and to emphasize the detection of specific metabolites but causes severe artifacts and an increase in spectral complexity in the HMBC experiment. To address this issue, the standard HMBC pulse sequence was modified to include carbon decoupling. Nonuniform sampling was also employed for rapid data collection. A dataset of reference 2D $^{1}H-^{13}C$ HMBC spectra was collected for 94 common metabolites. $^{13}C-^{13}C$ spin connectivity was then obtained by generating a covariance pseudo-spectrum from the carbon-decoupled HMBC and the $^{1}H-^{13}C$ HSQC−TOCSY spectra. The resulting $^{13}C-^{13}C$ pseudo-spectrum provides a connectivity map of the entire carbon backbone that uniquely describes each metabolite and would enable automated metabolite identification.

INTRODUCTION

Metabolomics is routinely used to describe phenotypic changes that occur in biological systems due to a variety of issues such as environmental stress, genetic modification, or a disease state.[1] NMR spectroscopy and mass spectrometry are the primary analytical platforms routinely employed to characterize these metabolomic changes.[2,3] The ability to accurately and efficiently identify the set of dysregulated metabolites from complex, heterogeneous biological or clinical samples is a fundamental challenge of all metabolomics studies.[4,5] NMR-based metabolomics studies have primarily relied on one-dimensional (1D) ^{1}H, two-dimensional (2D) $^{1}H-^{1}H$ total correlation spectroscopy (TOCSY), or 2D $^{1}H-^{13}C$-heteronuclear single quantum coherence (HSQC) experiments to analyze metabolomics samples.[6,7] Metabolite assignments are routinely accomplished by manually or semiautomatically matching experimental chemical shifts or peaks against spectral databases such as the human metabolome database (HMDB)[8] or Chenomx.[7] In this regard, the process of metabolite peak assignments is time-consuming, relatively primitive, and leaves ample room for unintentional mistakes or user bias.

Interpreting a 1D ^{1}H NMR spectrum is particularly cumbersome and error-prone because of the low chemical shift dispersion, the high peak overlap, and the large number of detectable (over a hundred) metabolites in a given spectrum.[9,10] ^{1}H chemical shifts are highly sensitive to changes in pH, temperature, salt, and the chemical composition of the metabolomics sample.[11] The resulting large chemical shift variance further complicates and confuses the chemical shift matching against reference databases. Accordingly, stable isotope labeling methods like stable isotope resolved metabolomics (SIRM) are commonly employed to incorporate ^{13}C-carbons into the metabolome by supplementing cell culture media with abundant nutrients, such as glucose,

Received: July 5, 2022
Accepted: November 4, 2022
Published: November 14, 2022

https://doi.org/10.1021/acs.analchem.2c02902
Anal. Chem. 2022, 94, 16308−16318

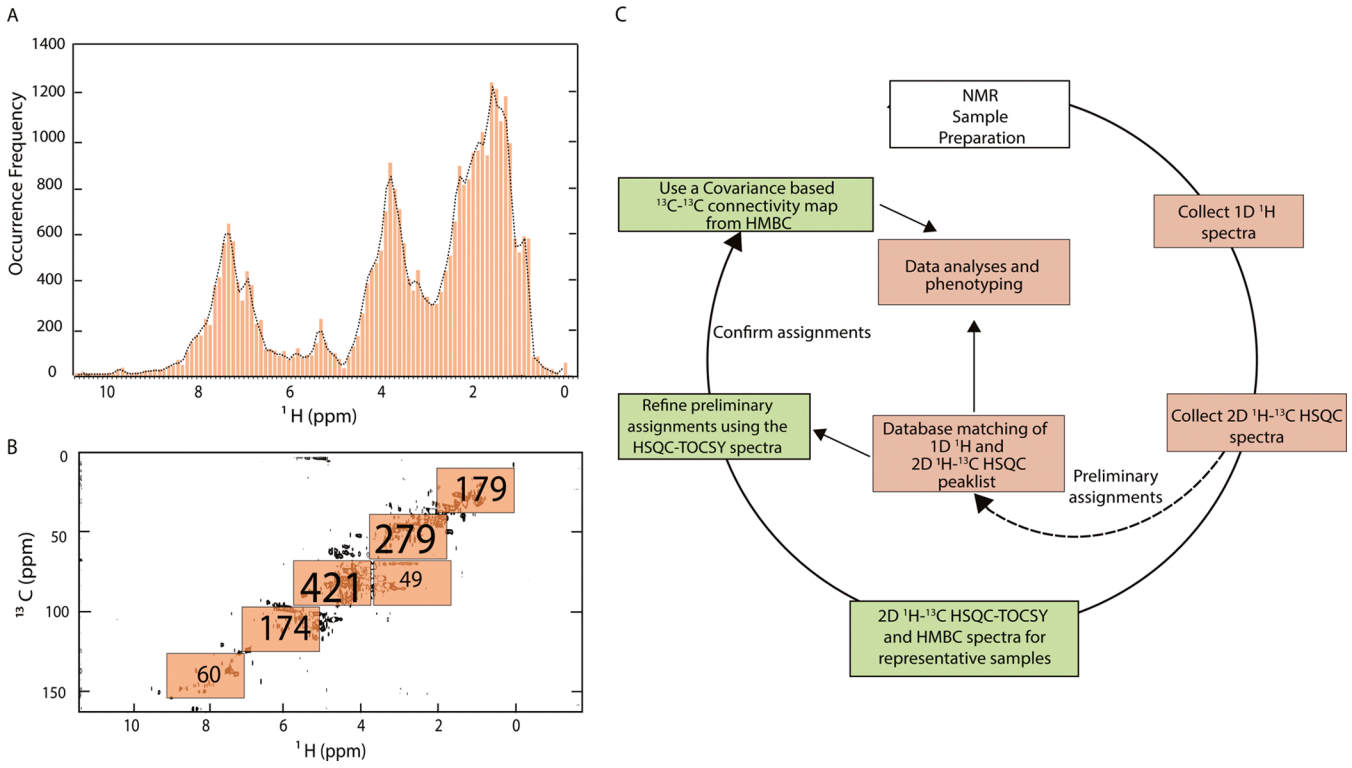

Figure 1. Chemical shift distribution of metabolites. (A) Bar graph summarizing the distribution of ^{1}H chemical shifts for the 1236 metabolites present in HMDB. A smooth curve is superimposed on the bar graph illustrating the general chemical shift trends. The bin size is 0.1 ppm. (B) Typical 2D ^{1}H−^{13}C HSQC spectrum obtained from an *E. coli* cell lysate. Overlaid on the NMR spectrum are bins with a dimension of 2 ppm in the ^{1}H dimension and 30 ppm in the ^{13}C dimension. The number in each bin corresponds to the number of metabolites from the BMRB database that have at least one chemical shift within the region defined by each bin. (C) Workflow of the NMR metabolite assignment protocol. The brown boxes correspond to the standard procedure based on matching chemical shifts from individual peaks to a database. The green boxes are our recommended additions to improve the assignment strategy.

amino acids, or acetate.[12−14] The 100-fold ^{13}C isotope enrichment enables the application of 2D ^{1}H−^{13}C HSQC experiments,[15] which has a significant advantage over a 1D ^{1}H spectrum due to the increased chemical shift dispersion and a decrease in chemical shift overlap. Additionally, the 2D ^{1}H−^{13}C HSQC experiment directly identifies correlated ^{1}H and ^{13}C chemical shifts, which both must match the database values to confirm an assignment. Having multiple, distinct, and correlated chemical shifts greatly increases the reliability of the metabolite assignment process. Despite these advantages, there are still concerns when it comes to peak identification and the uniqueness of each ^{1}H−^{13}C correlation in a 2D ^{1}H−^{13}C HSQC spectrum, particularly for crowded spectral regions. Multiple peaks from a single metabolite are commonly detected in a 2D ^{1}H−^{13}C HSQC spectrum, but reliably connecting these multiple HSQC peaks into a single spin system is not easily accomplished. It is also common for metabolites to be incompletely ^{13}C-labeled resulting in missing peaks in the 2D ^{1}H−^{13}C HSQC spectrum and incomplete spin systems.

Natural product chemists have recognized the value of a chemical identification workflow that incorporates multiple 2D NMR experiments.[16] A similar approach is slowly being adopted by the NMR metabolomics community to improve metabolite identification. For example, the COLMAR and MetaboMiner software uses 2D ^{1}H−^{1}H TOCSY, 2D ^{1}H−^{13}C HSQC, and HSQC−TOCSY spectra along with a spectral database (e.g., HMDB,[8] BMRB[17]). These software packages enable a semiautomated analysis of complex mixtures that improves the identification of metabolites.[18,19] Similarly, SpinCouple is a web-based tool that uses 2D ^{1}H−^{1}H J-resolved spectra and a database of about 600 metabolites to annotate metabolites that have a minimal number of peaks in a 2D ^{1}H−^{13}C HSQC spectrum.[20] A potential alternative method would combine the 2D ^{1}H−^{13}C heteronuclear multiple-bond correlation (HMBC)[21] experiment with the 2D ^{1}H−^{13}C HSQC and HSQC−TOCSY[22] experiments. In this manner, the 2D ^{1}H−^{13}C HMBC and HSQC−TOCSY experiments will provide nearly complete ^{1}H−^{13}C and ^{1}H−^{1}H spin systems, respectively, to connect with each HSQC peak. This approach would likely lead to an increase in the number of correlated chemical shifts, which would dramatically improve the accuracy of metabolite assignments. While databases of reference spectra include collections of both 1D (i.e., ^{1}H, ^{13}C, and DEPT) and 2D NMR experiments (i.e., 2D ^{1}H−^{13}C HSQC and 2D ^{1}H−^{1}H TOCSY), 2D ^{1}H−^{13}C HMBC spectra tend to be missing.[17,23−26]

The application of the 2D ^{1}H−^{13}C HMBC experiment to metabolomics presents some serious challenges: (1) HMBC is a low-sensitivity experiment, (2) the presence of additional ^{1}H−^{13}C peaks increases spectral crowding and leads to peak overlap, (3) heteronuclear J-coupling from ^{13}C isotope labeling will further deteriorate spectral quality and, (4) the large metabolite concentration range (from approximately 1−3 μM to upward of 1−5 M) presents a dynamic range problem that exacerbates the limited sensitivity of the HMBC experiment. These issues have prevented the wide adoption of the HMBC experiment by the metabolomics community. Herein, we

https://doi.org/10.1021/acs.analchem.2c02902
Anal. Chem. 2022, 94, 16308−16318

report a new strategy to improve the assignments of metabolites from complex biological samples by combining chemical shift data from the 2D $^{1}H-^{13}C$ HMBC, HSQC, and HSQC−TOCSY experiments. This effort included modifying a 2D $^{1}H-^{13}C$ HMBC pulse sequence to enable the analysis of ^{13}C-enriched samples, assembling a database of reference 2D $^{1}H-^{13}C$ HMBC spectra for 94 common metabolites, and utilizing 2D covariance matrix to simplify spectral analysis. Notably, the 2D covariance matrix is a pseudo-2D $^{13}C-^{13}C$ ADEQUATE (adequate sensitivity double quantum spectroscopy),[24] spectrum that provides a complete $^{13}C-^{13}C$ connectivity network that would be impractical to obtain experimentally. In this regard, the metabolite assignment strategy would exploit the spectral dispersion and the complete carbon connectivity offered by a covariance matrix that can be uniquely obtained from a decoupled HMBC spectrum. This is a first step toward automating metabolite assignments through pattern recognition.

MATERIAL AND METHODS

Analysis of Metabolite Chemical Shift Trends. 34 252 ^{1}H chemical shifts were compiled from the 1236 metabolites present in the HMDB[27] (http://www.hmdb.ca/downloads; accessed April 2019). The ^{1}H chemical shifts ranged from 0 to 11 ppm and were binned using a bin size of 0.1 ppm. The number of chemical shifts per bin was then plotted as the bar graph shown in Figure 1A. The BMRB database[2] (http://www.bmrb.wisc.edu/metabolomics/; accessed April 2019) contains correlated $^{1}H-^{13}C$ chemical shifts for 1159 metabolites. A representative 2D $^{1}H-^{13}C$ HSQC spectrum of an *Escherichia coli* metabolome extract was binned with a bin size equal to 2 ppm in the ^{1}H dimension and 30 ppm in the ^{13}C dimension. The bins were primarily restricted to the diagonal of the 2D $^{1}H-^{13}C$ HSQC spectrum, where the majority of the $^{1}H-^{13}C$ chemical shift correlations are located. The BMRB database was then searched to identify the number of unique metabolites with a chemical shift in each of the 2 ppm × 30 ppm bins. The 2 ppm × 30 ppm grid structure was superimposed onto the 2D $^{1}H-^{13}C$ HSQC spectrum (Figure 1B) where the number of uniquely assignable metabolites is indicated in each bin.

Preparation of Individual Metabolite Samples for NMR Analysis. NMR samples were prepared for each of the 18 metabolites listed in Table 1 and the 76 metabolites listed in Supporting Table 1S. A stock solution was prepared by dissolving each natural abundant metabolite to saturation in 1 mL of NANO Pure water (Barnstead, Dubuque, IA). NMR samples were prepared by diluting 10 μL of the stock metabolite solution with NANO Pure water to a final volume of 30 μL. The diluted metabolite solution was then added to 570 μL of a 50 mM phosphate buffer in D_2O (Cambridge Isotope Laboratories, Inc.) at pH 7.2 (uncorrected) for a final volume of 600 μL. The phosphate buffer solution contained 500 μM 3-(trimethylsilyl) propionic-2,2,3,3-d_4 acid sodium salt (98% D, TMSP) as an internal chemical shift reference and a concentration standard. The samples were then transferred to a 5 mm NMR tube for data collection.

Preparation of a Natural Abundance Metabolite Mixture for NMR Analysis. Approximately 1.3 μL of the stock solution for each of the 18 metabolites listed in Table 1 was combined to prepare a standard metabolomics mixture for NMR analysis. The standard metabolomics mixture was then diluted to a final volume of 600 μL by adding the required amount of a 50 mM phosphate buffer in D_2O at pH 7.2 (uncorrected). The phosphate buffer solution contained 500 μM TMSP as an internal chemical shift reference and concentration standard. In this manner, the total ionic strength of the NMR samples for the individual metabolites and the metabolomics mixture were identical. The standard metabolomics mixture was then transferred to a 5 mm NMR tube for data collection.

Table 1. Standard NMR Metabolomics Mixtures

no.	^{12}C-metabolites	^{13}C-metabolites
1	β-alanine	
2	L-arginine	$^{13}C_5$-L-arginine
3	L-asparagine	
4	L-glutamic acid	$^{13}C_5$-L-glutamic acid
5	L-glycine	$^{13}C_2$-L-glycine
6	L-lysine	
7	L-methionine	
8	L-phenylalanine	
9	L-proline	$^{13}C_5$-L-proline
10	L-serine	$^{13}C_2$-L-serine
11	L-threonine	$^{13}C_4$-L-threonine
12	L-tyrosine	
13	L-valine	
14	fructose	$^{13}C_6$-D-fructose
15	glucose	$^{13}C_6$-D-glucose
16	pyruvic acid	$^{13}C_2$-L-pyruvic acid
17	lactic acid	
18	L-alanine	$^{13}C_3$-L-alanine
19		$^{13}C_6$-L-leucine
20		$^{13}C_5$-L-glutamine

Preparation of ^{13}C-Labeled Metabolite Mixture for NMR Analysis. A 20 mM stock solution (100 μL) for each of the 12 ^{13}C-labeled metabolites listed in Table 1 was combined to prepare a standard NMR sample of a ^{13}C-labeled metabolomics mixture; 300 μL from the 1.2 mL ^{13}C-labeled metabolomics mixture was then diluted with 300 μL of a 50 mM phosphate buffer in D_2O at pH 7.2 (uncorrected) for a final volume of 600 μL. The final concentration for each ^{13}C-labeled metabolite in the mixture was 120 μM. The phosphate buffer contained 500 μM TMSP as an internal chemical shift reference and concentration standard. The ^{13}C-labeled metabolomics mixture was then transferred to a 5 mm NMR tube for data collection.

Preparation of Standard NMR Samples from Bacterial Metabolome Extracts. *E. coli* (strain MG1655) was cultured in M9 minimal media containing $^{13}C_2$ acetate (Isotec, Sigma-Aldrich) as the only carbon source. Triplicate 25 mL cell cultures were grown aerobically until a final OD_{600} of 36. The cells were harvested at the 12 h time-point upon reaching the stationary phase. Each cell culture was centrifuged at 5000 rpm for 20 min at 4 °C to pellet the cell suspension. Pellets were resuspended in 1.5 mL of 1:1 water/methanol solution. The cells were mechanically lysed by sonication using five 30 s intervals. The lysed cells were then centrifuged at 13 000 rpm for 20 min at 4 °C and 1 mL of the supernatant was transferred to a microcentrifuge tube. The metabolome cell extraction protocol was repeated, and the two supernatants were combined. The samples were kept on ice during the entire extraction process. Methanol was removed using a SpeedVac

https://doi.org/10.1021/acs.analchem.2c02902
Anal. Chem. 2022, 94, 16308−16318

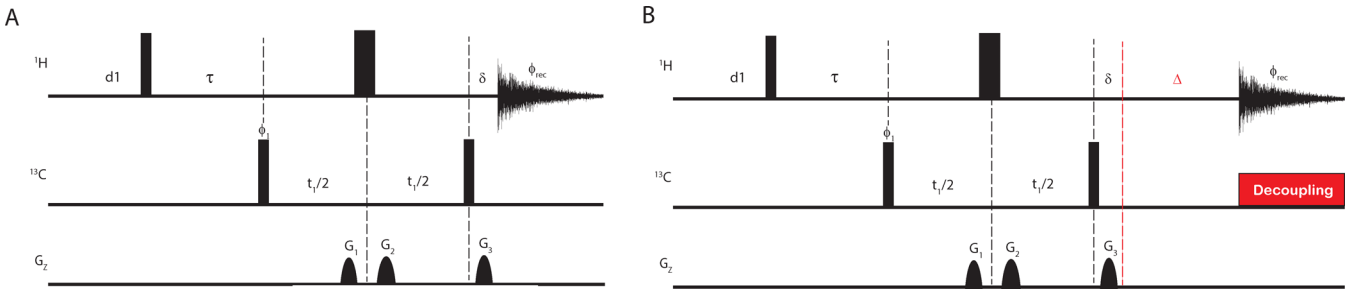

Figure 2. Pulse sequence diagrams. Schematic diagrams of (A) a standard Bruker HMBC (hmbcgpndqf) pulse sequence and (B) the ^{13}C-decoupled HMBC pulse sequence that includes the addition of a refocusing delay (Δ) equal to $0.5/(^{n}J_{CH}) + 0.5/(^{1}J_{CH})$ and ^{13}C decoupling applied during acquisition. Rectangle width and height represent pulse length and power levels. Delays (τ, δ, τ_1, Δ) are as labeled, and the durations are proportional to the relative lengths in the diagram. Gradients (G) were used as described in the original pulse sequence.[42] The changes to the HMBC pulse sequence are highlighted in red.

Plus SC110A system (Savant, Thermo Scientific), and the samples were then lyophilized using a FreeZone freeze dryer (Labconco, Kansas City, MO). The *E. coli* metabolome extracts were dissolved in 600 μL of 50 mM phosphate buffer at pH 7.2 (uncorrected) in D_2O and 500 μM TMSP. The samples were transferred to a 5 mm NMR tube for data collection.

NMR Pulse Sequence Development. *^{13}C-Decoupled HMBC Pulse Sequence.* The Bruker hmbcgpndqf pulse sequence was modified to include ^{13}C decoupling and a refocusing delay (Δ) prior to acquisition (Figure 2A,B). The refocusing delay equal to $0.5/(^{n}J_{CH}) + 0.5/(^{1}J_{CH})$ was added to an HMBC pulse program based on work done by Furihata and Seto[33] and later described by Furrer.[34] The $0.5/(^{n}J_{CH})$ term was set by the long-range C−H coupling constant (cnst13) in the pulse program. To get the desired HMBC $^{2}J_{CH}$ and $^{3}J_{CH}$ correlations, the long-range coupling constant was set between 6 and 10 Hz, with 8 Hz being a typical compromise. The $0.5/(^{1}J_{CH})$ term was set by the one-bond C−H coupling constant (cnst2) in the pulse program, typically set to 145 Hz.

NMR Data Collection and Processing. All NMR spectra were collected on a Bruker AVANCE III-HD 700 MHz spectrometer at 298 K using a 5 mm QCI-P inverse quadruple-resonance (^{1}H, ^{13}C, ^{15}N, ^{31}P) cryoprobe with cooled ^{1}H and ^{13}C channels and a *z*-axis gradient. All NMR spectra were processed using Topspin 3.6.2 and NMRPipe.[28] Spectra were processed with two zero-fills in each dimension, a sine-bell apodization function, and then Fourier-transformed. The spectra were manually analyzed in NMRviewJ (version 8.0, https://nmrfx.org/nmrfx/nmrviewj) to obtain lists of chemical shifts and peak intensities. Spectra were then converted into a text file using NMRPipe, which was transformed into a covariance matrix using a python script. The python script is provided in the accompanying Supporting Information.

2D ^{1}H−^{13}C−HMBC and the HSQC−TOCSY spectra of the ^{13}C-labeled *E. coli* metabolome extract were acquired with 2048 data points and a spectral width of 9090 Hz in the ^{1}H dimension and 128 data points and a spectral width of 38 735 Hz in the indirect ^{13}C dimension. The spectra were collected with 16 dummy scans, 16 scans, and a relaxation time of 1.5 s. The 2D ^{1}H−^{13}C HMBC spectrum of the standard ^{12}C-metabolite mixture was acquired with 1024 data points and a spectral width of 11 160.74 Hz in the ^{1}H dimension and 64 data points and a spectral width of 38 735 Hz in the indirect ^{13}C dimension. The spectra were collected with 16 dummy scans, 16 scans, and a relaxation time of 1.5 s. The acquisition was repeated using nonuniform sampling at 50% sparsity with our deterministic schedular.[29]

A database of individual 2D ^{1}H−^{13}C−HMBC spectra for the 94 metabolites listed in Tables 1 and S1 was assembled by acquiring the HMBC spectra with nonuniform sampling. The spectra were acquired using our deterministic sampling scheme[30] at a 50% sparsity and then processed following multidimensional deconvolution (MDD)[31] reconstruction as implemented in Bruker Topspin version 3.6.2. The 2D ^{1}H−^{13}C HMBC spectra of the individual metabolites were acquired with the identical parameters used for the *E. coli* metabolome extract except the number of scans was doubled to account for the fact that the metabolites were not ^{13}C-labeled. The 2D ^{1}H−^{13}C HMBC spectrum for the *E. coli* metabolome extract was collected with both uniform and no-uniform sampling.

A 2D ^{1}H−^{13}C−(1, *n*) ADEQUATE spectrum of a standard 1 mM glucose sample was collected using the adeq11etgprdsp pulse sequence. The 2D ^{1}H−^{13}C−(1, *n*) ADEQUATE spectrum was acquired with 2048 data points and a spectral width of 9090 Hz in the ^{1}H dimension and 256 data points and a spectral width of 36 986 Hz in the indirect ^{13}C dimension. The 2D ^{1}H−^{13}C−(1, *n*) ADEQUATE experiment was collected with 16 dummy scans, 64 scans, and a relaxation delay of 1.5 s.

2D Covariance Matrix. Denote a 2D^{1}H−^{13}C HMBC spectrum by an $N_1 \times N_2$ matrix X. The ^{13}C−^{13}C covariance matrix represented by C is obtained as follows

$$C = (X^T X)^{1/2}$$

where X^T is a transpose matrix of X. The resulting covariance matrix C has dimensions of $N_2 \times N_2$. Each off-diagonal element of C, referred to as a cross-peak, represents a correlation between two corresponding carbon resonances across all proton resonances in X. A more intense cross-peak indicates that the two corresponding carbons share more common proton resonances. In essence, the covariance matrix C removes the ^{1}H dimension while highlighting the carbon−carbon connectivities.

RESULTS AND DISCUSSION

Limited Chemical Shift Dispersion Is a Challenge to Metabolite Assignments. An integral part of any metabolomics project, and by far the most time-consuming aspect of the process, is metabolite assignments. Untargeted NMR metabolomics commonly relies on 1D ^{1}H NMR spectral

https://doi.org/10.1021/acs.analchem.2c02902
Anal. Chem. 2022, 94, 16308−16318

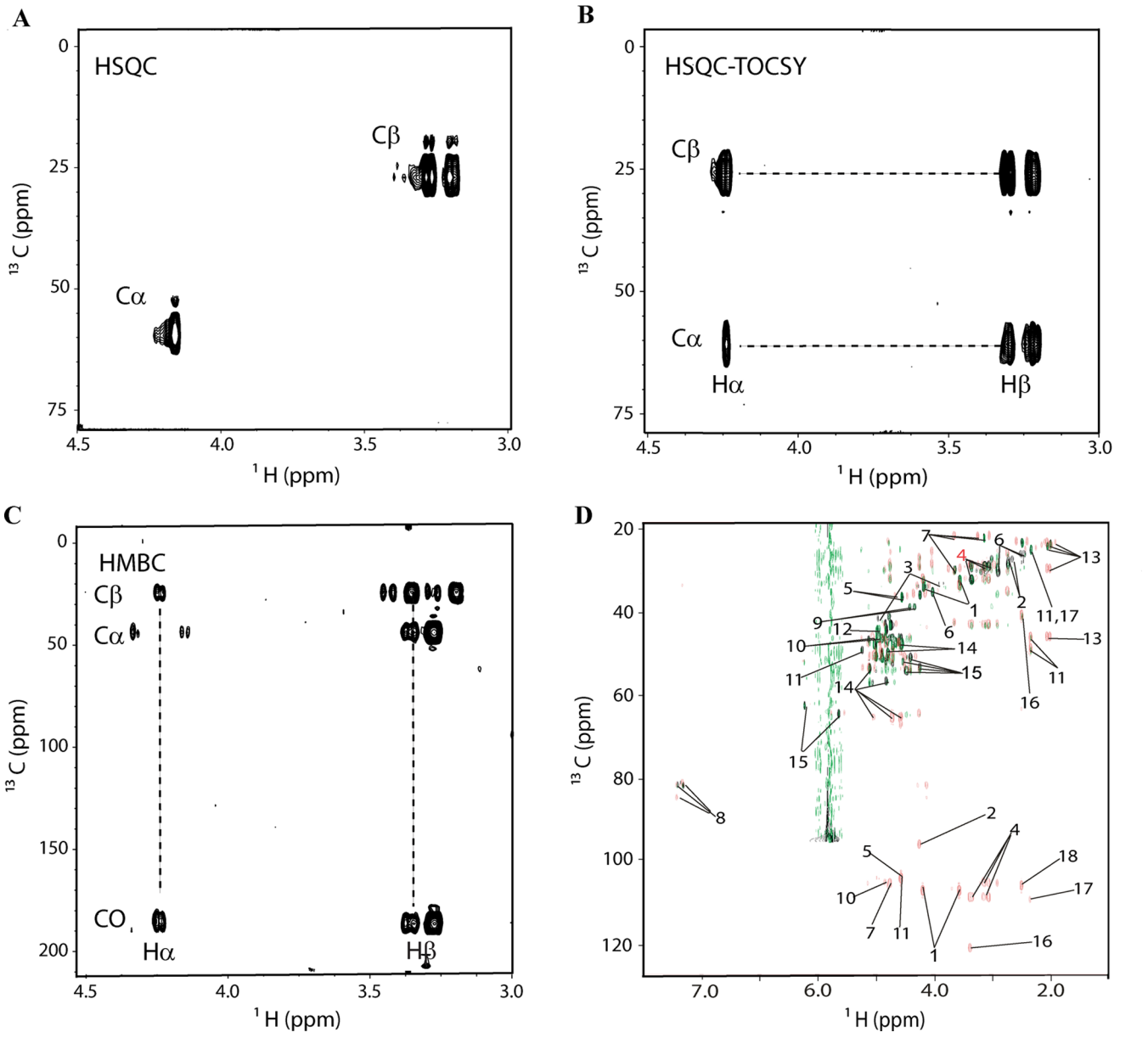

Figure 3. Representative 2D NMR dataset for metabolite assignments. Expanded views of the (A) 2D ^{1}H−^{13}C HSQC, (B) 2D ^{1}H−^{13}C HSQC−TOCSY, and (C) 2D ^{1}H−^{13}C HMBC spectra for the metabolite L-asparagine. The spectra were collected using a natural abundant L-asparagine sample. The spectra are annotated to identify the carbon (Cα, Cβ), hydrogen (Hα, Hβ), and carbonyl (CO) chemical shifts and the TOCSY and HMBC correlations. (D) Spectral overlay of a 2D ^{1}H−^{13}C HSQC (black), 2D ^{1}H−^{13}C HSQC−TOCSY (green), and 2D ^{1}H−^{13}C HMBC (orange) spectrum for the standard ^{12}C-metabolite mixture. The metabolite assignments are indicated as listed in Table 1. Individual reference spectra for each metabolite, as illustrated in (A−C), were used to make the assignments.

information to characterize metabolome differences and to identify metabolite changes. 1D ^{1}H NMR spectra are remarkably data-rich, and when thoroughly analyzed, are highly informative. Nevertheless, interpreting 1D ^{1}H NMR spectra is still challenged by the limited chemical shift range (Figure 1A), and by the fact that peak position is impacted by variations in sample conditions (e.g., pH). As a result, there may be a high level of ambiguity in assigning a complex 1D ^{1}H NMR spectrum derived from a heterogeneous biological mixture. Well-designed metabolomics studies routinely include representative 2D NMR spectra to aid in metabolite assignments and to improve the accuracy of the identification process.[32] Simply, ^{1}H chemical shifts are spread out into two dimensions. A common approach is the use of traditional 2D ^{1}H−^{1}H TOCSY and COSY experiments.[23]

A search of NMR metabolomics databases shows that certain spectral regions are heavily populated. The distribution of ^{1}H chemical shifts for the 1236 metabolites in the HMDB[27] shown in Figure 1A indicates abundant clusters around 1.75, 4, and 7.5 ppm. This limited distribution of metabolite ^{1}H chemical shifts makes the analysis of even 2D ^{1}H NMR experiments challenging since most of the observed chemical shift coherence would be restricted to these densely occupied regions. Further increasing the spectral resolution is routinely achieved by leveraging the larger carbon chemical shift window by obtaining ^{1}H−^{13}C chemical shift correlations observed in a 2D ^{1}H−^{13}C HSQC spectrum. Coupled ^{1}H−^{13}C chemical

https://doi.org/10.1021/acs.analchem.2c02902
Anal. Chem. 2022, 94, 16308−16318

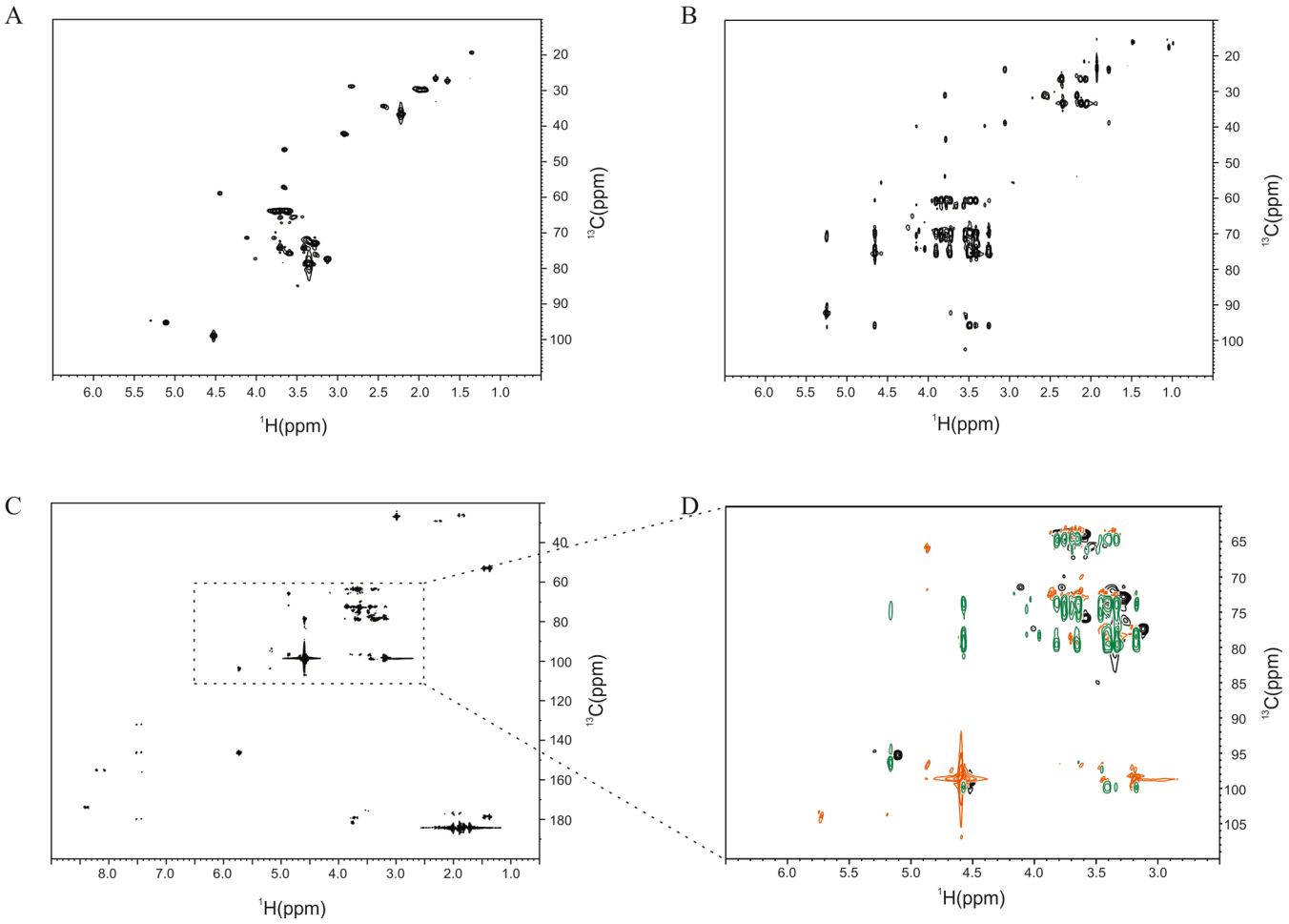

Figure 4. NMR spectra of the *E. coli* metabolome. (A) 2D ^{1}H−^{13}C HSQC, (B) 2D ^{1}H−^{13}C HSQC−TOCSY, and (C) 2D ^{13}C-decoupled HMBC spectra of the metabolome extracted from an *E. coli* cell lysate labeled with $^{13}C_2$ acetate. (D) Spectral overlay of the 2D ^{1}H−^{13}C HSQC (black), 2D ^{1}H−^{13}C HSQC−TOCSY (green), and 2D ^{13}C-decoupled HMBC (orange) spectra corresponding to the expansion of the carbohydrate region shown in (C).

shifts are also highly correlated such that most peaks observed in an HSQC spectrum fall along a diagonal. The relative distribution of ^{1}H and ^{13}C chemical shifts for a typical metabolome extract is shown in Figure 1B. Superimposed onto this spectrum are chemical shift bins positioned along the diagonal. The number of metabolites from the BMRB database that have a chemical shift that falls within each binned region is indicated. ^{1}H−^{13}C chemical shift pairs for common metabolites are restricted to small regions centered around the diagonal. A majority of metabolites cluster in a grid around 3 to 6 and 50 to 80 ppm. Since a significant amount of the 2D ^{1}H−^{13}C HSQC spectrum is empty space, especially off the diagonal, this presents an opportunity to include longer-range correlations since the 2D ^{1}H−^{13}C HSQC experiment only provides one-bond hydrogen−carbon correlations through $^{1}J_{CH}$.

Metabolomics investigators have routinely used 2D ^{1}H−^{13}C HSQC experiments to characterize metabolome changes, but there is a clear value in extending the approach to include multiple 2D NMR experiments. Multiple 2D NMR experiments will increase the confidence and reliability of metabolite identification and aid in the development of automating metabolite identification. Natural product investigators have developed and utilized an array of 2D NMR experiments, such as HMBC,[21] long-range heteronuclear single quantum multiple-bond correlation (LR-HSQMBC),[33] ADEQUATE,[24] and incredible natural abundance double quantum transfer experiment (INADEQUATE).[16,24] Different connectivity and structural information is acquired from each of these NMR methods, which may be critical to moving the metabolomics field forward by enhancing the 2D ^{1}H−^{13}C HSQC approach. In this regard, the 2D ^{1}H−^{13}C HMBC experiment is important for establishing two- to four-bond ^{13}C connectivity, especially between methyl, methylene, and methine groups that are separated by quaternary carbons or heteroatoms. Chemical bonds between heteroatoms and carbons are a structural feature common to metabolites involved in central carbon metabolism.

Leveraging 2D Spectra to Facilitate Metabolite Assignments. A common approach to assigning metabolites from a biological sample is to peak-fit a 1D ^{1}H spectrum with reference spectra (i.e., Chenomx approach) or to generate a complete peak list from a 2D ^{1}H−^{13}C HSQC and match to a chemical shift database. An expert must refine the metabolite assignments based on several parameters, such as (i) spin system completeness, (ii) metabolic pathway completeness, (iii) removing multiple assignments to the same chemical shifts, (iv) knowledge about the cell or organism's specific metabolism, and (v) consistency with secondary NMR

https://doi.org/10.1021/acs.analchem.2c02902
Anal. Chem. 2022, 94, 16308−16318

experiments (e.g., 2D $^{1}H-^{1}H$ COSY and TOCSY). There is a potential bias to this process since it is extremely reliant on the expert's knowledge and experience. The current workflow needs to evolve toward an automated process that uses an iterative and layered approach involving multiple 2D spectra. Simply, the standard protocol (Figure 1C) is appended by including 2D $^{1}H-^{13}C$ HSQC−TOCSY and HMBC spectra. An initial list of potential metabolites is still obtained by peak matching the 2D $^{1}H-^{13}C$ HSQC spectrum against reference databases. Representative 2D $^{1}H-^{13}C$ HSQC−TOCSY and HMBC spectra are then used to create complete spin systems. The 2D $^{1}H-^{13}C$ HSQC-derived list of potential metabolites is filtered by the collection of identified spin systems. Both the assignment step and filtering step are amenable to automation. The 2D $^{1}H-^{13}C$ HSQC−TOCSY and HMBC spectra may be converted into a complete $^{13}C-^{13}C$ connectivity map that can be combined with graph theory to complete the spin system assignments, as discussed below.

An illustration of the proposed approach is shown in Figure 3. 2D $^{1}H-^{13}C$ HSQC, HSQC−TOCSY, and HMBC spectra were collected for asparagine (Figure 3A−C). The availability of multiple distinct spectral data for each individual metabolite greatly improves the accuracy of metabolite assignments. Simply, a metabolite assignment based on a complete spin system, which contains numerous chemical shifts and connectivity patterns, is highly likely to be correct relative to matching a few or one chemical shift to existing databases. The 2D $^{1}H-^{13}C$ HSQC spectra illustrated in Figure 3A are a common resource for metabolite assignments since in principle it contains the full $^{1}H-^{13}C$ spin system for a metabolite, but it lacks connectivity information. This is not an issue for an isolated compound, but in a complex mixture, like Figure 3D, identifying which peaks are associated with a specific spin system or metabolite can be a daunting endeavor. The companion 2D $^{1}H-^{13}C$ HSQC−TOCSY, and HMBC spectra address this issue. For example, the 2D $^{1}H-^{13}C$ HSQC−TOCSY spectrum in Figure 3B connects the entire asparagine $^{1}H-^{13}C$ spin system through coupled ^{1}Hs. The 2D $^{1}H-^{13}C$ HMBC spectra in Figure 3C provide further information through long-range $^{13}C-^{13}C$ coupling that can connect to unprotonated carbons missed in both the 2D $^{1}H-^{13}C$ HSQC and HSQC−TOCSY experiments. A correlation to the carbonyls is seen for asparagine, which provides further information to correctly identify the metabolite. Acquiring both the 2D $^{1}H-^{13}C$ HSQC and HSQC−TOCSY is still important despite some redundancy in information content because of spectral complexity and peak overlap common to a complex, heterogeneous mixture. Simply, information obscured in one spectrum may be observable in the other. Using this approach, the entire standard mixture of 18 compounds in Table 1 was completely and easily assigned by a novice (Figure 3D). The same approach would be employed to assign the more complex spectra depicted in Figure 4 of the ^{13}C-labeled metabolome extracted from *E. coli* lysate.

Database of 2D $^{1}H-^{13}C$ HMBC Spectra for Common Metabolites. The HMDB, BMRB, and other NMR reference databases are populated with multiple 1D ^{1}H, 2D $^{1}H-^{1}H$ (typically COSY and TOCSY), and 2D $^{1}H-^{13}C$ (typically HSQC) spectra. Nevertheless, expanding and enhancing these databases by acquiring other 2D NMR spectra, such as the 2D $^{1}H-^{13}C$ HSQC−TOCSY and 2D $^{1}H-^{13}C$ HMBC, are still needed to enable the assignment protocol as outlined in Figure 1C. To date, we have collected 282 2D NMR spectra for the 94 metabolites listed in Table S1. A set of representative 2D $^{1}H-^{13}C$ HSQC, HSQC−TOCSY, and HMBC spectra are shown in Figure 3A−C. The availability of such a set of reference data will help facilitate the routine, automatic assignment of known metabolites. Nevertheless, a major obstacle to employing the 2D $^{1}H-^{13}C$ HMBC experiment in metabolomics is the common use of ^{13}C-enriched samples.

^{13}C-Decoupled HMBC Pulse Sequence for Metabolomics. The Bruker HMBC (hmbcgpndqf) pulse sequence without a filter yielded a crowded spectrum for the ^{13}C-labeled *E. coli* metabolome extract (Figure S1A). The spectrum was populated with numerous $^{13}C-^{13}C$ coupled peaks and was clearly unusable. The HMBC pulse sequences with low-pass filters (hmbcetgpl1nd, hmbcetgpl2nd, hmbcgpl3nd) were then compared to identify a pulse sequence that provided a quality spectrum from a fully ^{13}C-labeled cell lysate. Unfortunately, all the HMBC pulse sequences with a low-pass filter resulted in a loss of peak intensity while $^{13}C-^{13}C$ coupled peaks were still present in the spectra (Figure S1B). Interestingly, the loss in peak intensity occurred in different regions of the spectrum. As a result, the available HMBC pulse sequences were determined to be unacceptable for the analysis of ^{13}C-labeled metabolomics samples. To resolve this issue, an existing HMBC pulse program (hmbcgpndqf) was edited to include ^{13}C-nuclei decoupling during acquisition. The detailed pulse sequence for the coupled and decoupled 2D $^{1}H-^{13}C$ HMBC experiment are shown in Figure 2A,B, respectively. A ^{13}C-decoupled HMBC pulse sequence was first described to be used in natural product structure elucidation by Furihata et al.[34]

Incorporating ^{13}C decoupling into the HMBC pulse sequence yielded a poor-quality 2D $^{1}H-^{13}C$ HMBC spectrum (data not shown). The loss of HMBC cross-peaks when applying ^{13}C decoupling was previously explained by Furrer[35] when describing the work of Furihata et al.[34] The classical HMBC pulse sequence yields antiphase cross-peaks, which results in cross-peak cancelation when ^{13}C decoupling is used during acquisition. HMBC cross-peaks can be restored by the addition of a refocusing delay (Δ) before the ^{13}C-decoupled acquisition.[34] The refocusing delay converts the antiphase cross-peaks into in-phase. The downside is the possible loss of signal due to T_2 relaxation during the approximate 60 ms refocusing delay.

To illustrate the utility of ^{13}C-decoupled HMBC for metabolite assignment, 2D $^{1}H-^{13}C$ NMR spectra, including ^{13}C-decoupled HMBC, were acquired on an *E. coli* cell lysate ^{13}C-metabolome extract (Figure 4). It is important to note that the spectra were collected with NUS at a 50% sparsity to decrease the overall experiment time and improve sensitivity. A further reduction in experiment time may be possible by also implementing the SOFAST technique.[36] The 2D $^{1}H-^{13}C$ HSQC (Figure 4A) and 2D $^{1}H-^{13}C$ HSQC−TOCSY (Figure 4B) spectra show results typical of such a sample, without problems arising from $^{13}C-^{13}C$ coupling. Compared with just a 2D $^{1}H-^{13}C$ HSQC spectrum, spectral overlays of the 2D $^{1}H-^{13}C$ HSQC−TOCSY and the ^{13}C-decoupled HMBC (Figure 4C,D) spectra show additional correlations that aid in metabolite assignments. Accordingly, the ^{13}C-decoupled HMBC should be a valuable resource for the metabolomics community and will enable NMR spectroscopists to include an additional experiment as part of a routine workflow to facilitate metabolite assignments.

https://doi.org/10.1021/acs.analchem.2c02902
Anal. Chem. 2022, 94, 16308−16318

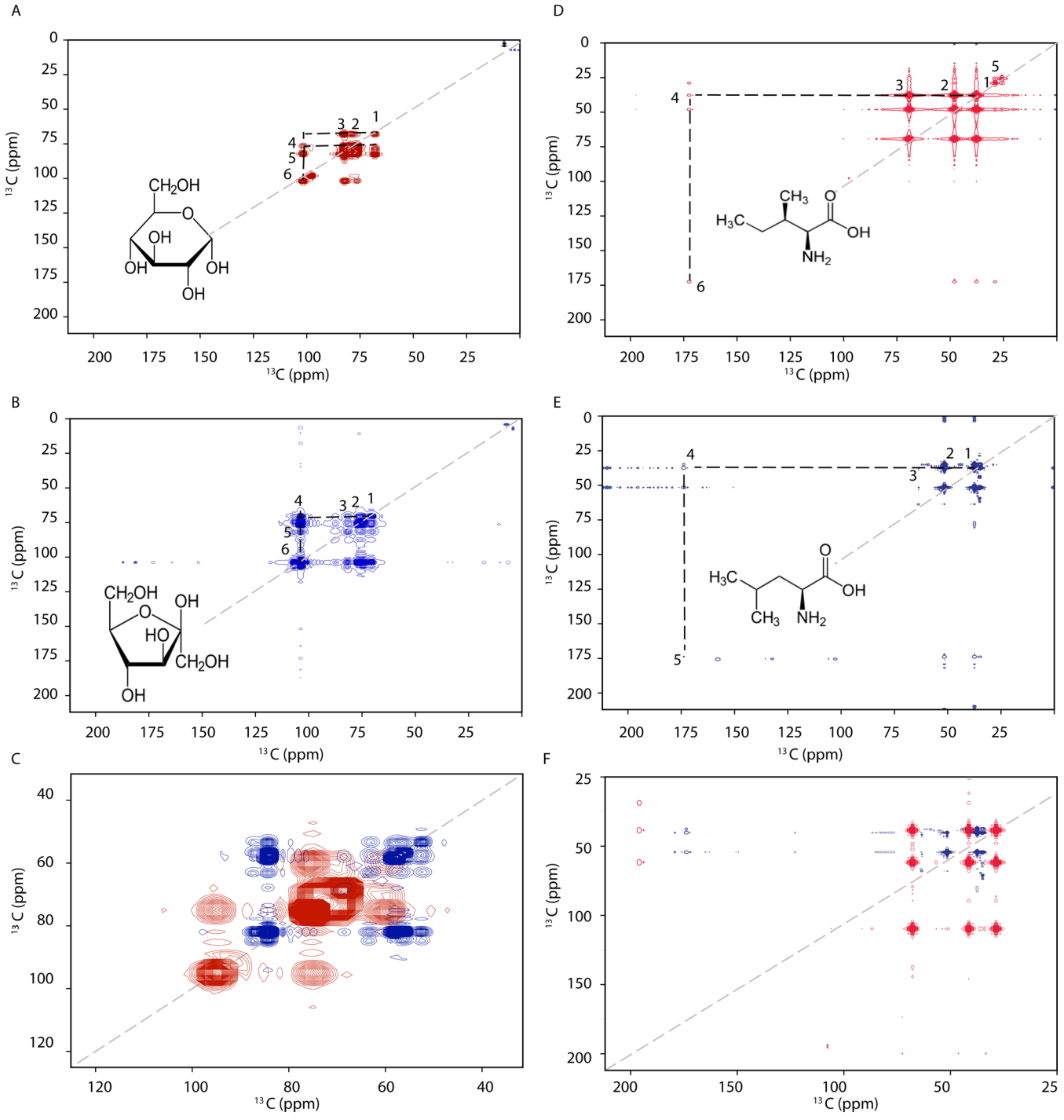

Figure 5. Illustrative HMBC-derived $^{13}C-^{13}C$ covariance pseudo-spectra. $^{13}C-^{13}C$ covariance pseudo-spectrum of (A) glucose, (B) fructose, (D) leucine, and (E) isoleucine. The chemical structures are included as an inset. The $^{13}C-^{13}C$ connectives are numbered and connected by dashed lines. (C) Overlay of zoomed regions from the fructose and glucose $^{13}C-^{13}C$ covariance spectra from (A, B). (F) Overlay of zoomed regions from the leucine and isoleucine $^{13}C-^{13}C$ covariance spectra from (D, E).

HMBC Covariance Spectra and Confident Metabolite Assignments. Obtaining a complete $^{13}C-^{13}C$ connectivity map for each spin system would be invaluable for achieving the complete and accurate identification of every metabolite in a complex biological mixture. Unfortunately, ^{1}H NMR is approximately 5720 times more sensitive than ^{13}C because of the low natural abundance of ^{13}C-carbons (1.1%) and its smaller gyromagnetic ratio. Thus, experimentally observing $^{13}C-^{13}C$ coupling suffers from extremely low sensitivity and long acquisition times, which makes it impractical for most large-scale metabolomics studies. Conversely, a ^{13}C-decoupled HMBC spectrum collected on ^{13}C-enriched or naturally abundant metabolomics samples can be easily used to indirectly obtain a complete $^{13}C-^{13}C$ connectivity map. Simply, a covariance matrix can be generated from a 2D $^{1}H-^{13}C$ HMBC spectrum that exhibits the same $^{13}C-^{13}C$ connectivity observed in an experimental 2D $^{13}C-^{13}C$ INADEQUATE spectrum.[37] The HMBC-derived covariance

https://doi.org/10.1021/acs.analchem.2c02902
Anal. Chem. 2022, 94, 16308−16318

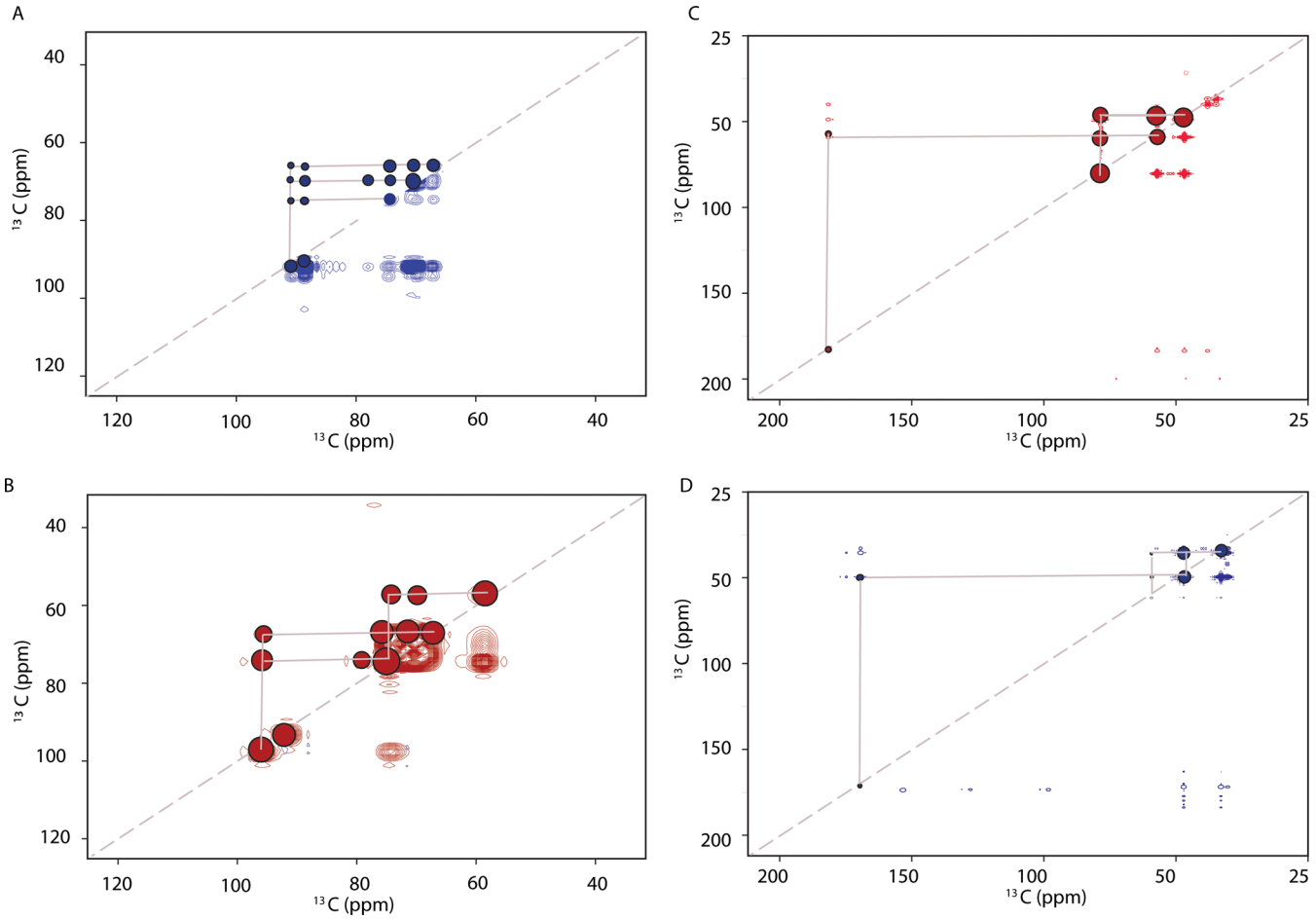

Figure 6. Illustrative graphs from HMBC-derived $^{13}C-^{13}C$ covariance pseudo-spectra. Expanded views of the $^{13}C-^{13}C$ covariance pseudo-spectra from Figure 5 are overlaid with graphs for (A) fructose, (B) glucose, (C) leucine, and (D) isoleucine. Each of the filled circles represents a cross-peak or carbon node that is part of the $^{13}C-^{13}C$ connectivity map. The size of the circles represents the relative intensity of the peaks as observed in the 2D HMBC spectrum.

spectrum for a few select metabolites is shown in Figure 5. More specifically, Figure 5A shows the cross-peaks between C1 (74 ppm) and C2 (75 ppm), C3 (78 ppm) as these three carbons share some common ^{1}H peaks between 3.3 and 3.8 ppm. Additional cross-peaks between C6 (100.2 ppm), C5 (80 ppm), and C4 (75.2 ppm) are also observed. Similar interpretations can be extended to Figure 5B,D,E. Close inspection of the $^{13}C-^{13}C$ covariance pseudo-spectra of the structurally similar metabolites, glucose (Figure 5A) and fructose (Figure 5B), clearly identifies two distinct connectivity maps. The overlay of the two spectra in Figure 5C further illustrates how the two metabolites are uniquely identifiable.

The $^{13}C-^{13}C$ covariance pseudo-spectra for leucine and isoleucine is shown in Figure 5D,E, respectively. Both amino acids are commonly present in metabolomics samples and are an important measure of branched-chain amino acid metabolism. These amino acids present an assignment challenge due to the limited chemical shift differences in 1D ^{1}H or 2D $^{1}H-^{13}C$ HSQC spectra. An accurate identification, even by an expert, may be unreliable. Conversely, the overlay of the two covariance spectra in Figure 5F clearly demonstrates their unique connectivity maps. Accordingly, an unambiguous assignment for leucine and isoleucine can be easily made by a novice. These $^{13}C-^{13}C$ covariance matrices clearly illustrate the potential utility of the ^{13}C-decoupled HMBC spectrum to aid in the accurate and automated assignments of metabolites. A 2D $^{1}H-^{13}C$ HMBC experiment requires less than 10% of the time necessary to collect a 2D $^{1}H-^{13}C$ ADEQUATE, and less than 5% of the time required for a 2D $^{13}C-^{13}C$ INADEQUATE spectrum of reasonable quality.[38] In essence, the 2D $^{13}C-^{13}C$ pseudo-spectrum generated from the 2D $^{1}H-^{13}C$ HMBC spectrum may save days of NMR time while providing the same information.

HMBC Covariance Spectra Enables Automated Metabolite Assignments Using Graph Theory. NMR metabolomics relies on a tedious assignment process based on the manual peak matching between multiple NMR spectra and database searches. An automated and reliable workflow is an unmet need of the metabolomics community. Combining the HMBC-derived $^{13}C-^{13}C$ connectivity maps with Graph theory may provide a path to automation. Graph theory has been previously applied to solve protein backbone sequential assignments and to assign ^{13}C chemical shifts in alkanes.[39−41] In essence, each 2D NMR spectrum is converted into a graph (G) where peaks are the vertices (V) and the distance between peaks are edges (E). Example bipartite graphs, $G(V, E)$, that result from the reduction of experimental 2D $^{13}C-^{13}C$ pseudo-spectra are illustrated in Figure 6. The combination of weights (from peak intensity), vertices (from peak positions), and edges (from peak-to-peak distances) presents a unique

https://doi.org/10.1021/acs.analchem.2c02902
Anal. Chem. 2022, 94, 16308−16318

bipartite graph for each metabolite that can be matched in its entirety. The 2D $^{13}C-^{13}C$ pseudo-spectra from Figure 5 were overlaid with a bipartite graph illustrating the unique patterns for fructose (Figure 6A), glucose (Figure 6B), leucine (Figure 6C), and isoleucine (Figure 6D). In this manner, these HMBC-derived graphs may replace individual peak matching by matching the entire spin system, which would be expected to provide robust MSI-level 1 assignments.

CONCLUSIONS

The value of multidimensional pulse sequences to NMR-based metabolomics is undeniable. Moreover, they provide a potential framework to automate the assignment process. In the context of a metabolomics workflow, the 2D $^{1}H-^{13}C$ HMBC and the 2D $^{1}H-^{13}C$ HSQC−TOCSY pulse sequences present an attractive approach. It is routinely used by natural product investigators, works with standard hardware, takes advantage of higher ^{1}H sensitivity, and can be acquired in the short time frame necessary for high-throughput metabolomics. A major obstacle is the fact that metabolomics samples are routinely ^{13}C-labeled, which yields unusable spectra with available 2D $^{1}H-^{13}C$ HMBC pulse sequences. We described the use of a ^{13}C-decoupled HMBC pulse sequence and assembled an initial database of 2D $^{1}H-^{13}C$ HMBC reference spectra for 94 common metabolites. The addition of the ^{13}C-decoupled HMBC experiment to a standard metabolomics workflow will improve the reliability of metabolite assignments from complex mixtures. Automated, accurate metabolite assignment is a current challenge for NMR metabolomics. 2D $^{1}H-^{13}C$ HSQC and $^{1}H-^{1}H$ TOCSY methods lack an efficient and rapid means of assembling entire metabolite spin systems. However, the 2D $^{1}H-^{13}C$ HSQC−TOCSY allows for the assignment of hydrogen-rich metabolites. The metabolite assignment process may progress to a fully automated operation by incorporating our strategy of using a $^{13}C-^{13}C$ covariance matrix that is easily generated from a ^{13}C-decoupled HMBC and the 2D $^{1}H-^{13}C$ HSQC−TOCSY spectrum. An HMBC-derived $^{13}C-^{13}C$ covariance matrix combined with graph theory holds great promise for an automated approach to metabolite assignments.

ASSOCIATED CONTENT

Supporting Information

The Supporting Information is available free of charge at https://pubs.acs.org/doi/10.1021/acs.analchem.2c02902.

Table listing the 94 metabolites used to collect 2D NMR spectra; figures of representative standard 2D $^{1}H-^{13}C$ HMBC spectra obtained for ^{13}C-labeled metabolome extracted from *E. coli*; and Bruker NMR pulse sequences for the (1) ^{13}C-decoupled HMBC sequence with an added delay before acquisition and (2) ^{13}C-decoupled HMBC sequence with low-pass filter (PDF)

AUTHOR INFORMATION

Corresponding Author

Robert Powers − *Department of Chemistry, University of Nebraska-Lincoln, Lincoln, Nebraska 68588-0304, United States; Nebraska Center for Integrated Biomolecular Communication, University of Nebraska-Lincoln, Lincoln, Nebraska 68588-0304, United States;* orcid.org/0000-0001-9948-6837; Phone: (402) 472-3039; Email: rpowers3@unl.edu; Fax: (402) 472-9402

Authors

Fatema Bhinderwala − *Department of Chemistry, University of Nebraska-Lincoln, Lincoln, Nebraska 68588-0304, United States; Nebraska Center for Integrated Biomolecular Communication, University of Nebraska-Lincoln, Lincoln, Nebraska 68588-0304, United States; Department of Structural Biology, University of Pittsburgh School of Medicine, Pittsburgh, Pennsylvania 15213-3301, United States*

Thao Vu − *Department of Statistics, University of Nebraska-Lincoln, Lincoln, Nebraska 68583-0963, United States; Department of Biostatistics and Informatics, Colorado School of Public Health, University of Colorado Anschutz Medical Campus, Aurora, Colorado 80045-2609, United States*

Thomas G. Smith − *Department of Chemistry, University of Nebraska-Lincoln, Lincoln, Nebraska 68588-0304, United States; Nebraska Center for Integrated Biomolecular Communication, University of Nebraska-Lincoln, Lincoln, Nebraska 68588-0304, United States*

Julian Kosacki − *Department of Chemistry, University of Nebraska-Lincoln, Lincoln, Nebraska 68588-0304, United States*

Darrell D. Marshall − *Department of Chemistry, University of Nebraska-Lincoln, Lincoln, Nebraska 68588-0304, United States*

Yuhang Xu − *Department of Statistics, University of Nebraska-Lincoln, Lincoln, Nebraska 68583-0963, United States; Department of Applied Statistics and Operations Research, Bowling Green State University, Bowling Green, Ohio 43403-0001, United States*

Martha Morton − *Department of Chemistry, University of Nebraska-Lincoln, Lincoln, Nebraska 68588-0304, United States; Nebraska Center for Integrated Biomolecular Communication, University of Nebraska-Lincoln, Lincoln, Nebraska 68588-0304, United States;* orcid.org/0000-0002-6411-1733

Complete contact information is available at: https://pubs.acs.org/10.1021/acs.analchem.2c02902

Author Contributions

F.B., D.D.M., and R.P. conceived the project. F.B., T.G.S., J.K., D.D.M., and M.M. performed the experiments. F.B. and T.V. processed the data for covariance spectrum. F.B., D.D.M., R.P., and M.M. designed the experiments. F.B., M.M., and R.P. analyzed the data and wrote the manuscript.

Notes

The authors declare no competing financial interest.

ACKNOWLEDGMENTS

This work was supported by the National Science Foundation under Grant Number (1660921) and, in part by funding from the Redox Biology Center (P30 GM103335, NIGMS), and the Nebraska Center for Integrated Biomolecular Communication (P20 GM113126, NIGMS). The research was performed in facilities renovated with support from the National Institutes of Health (RR015468-01). Any opinions, findings, and conclusions or recommendations expressed in this material are those of the author(s) and do not necessarily reflect the views of the National Science Foundation.

REFERENCES

(1) Gebregiworgis, T.; Powers, R. *Comb. Chem. High Throughput Screening* **2012**, *15*, 595−610.
(2) Markley, J. L.; Brüschweiler, R.; Edison, A. S.; Eghbalnia, H. R.; Powers, R.; Raftery, D.; Wishart, D. S. *Curr. Opin. Biotechnol.* **2017**, *43*, 34−40.
(3) Marshall, D. D.; Powers, R. *Prog. Nucl. Magn. Reson. Spectrosc.* **2017**, *100*, 1−16.
(4) Johnson, C. H.; Gonzalez, F. J. *J. Cell. Physiol.* **2012**, *227*, 2975−2981.
(5) Nagana Gowda, G. A.; Raftery, D. *J. Magn. Reson.* **2015**, *260*, 144−160.
(6) Bhinderwala, F.; Lonergan, S.; Woods, J.; Zhou, C.; Fey, P. D.; Powers, R. *Anal. Chem.* **2018**, *90*, 4521−4528.
(7) Bingol, K.; Li, D.-W.; Bruschweiler-Li, L.; Cabrera, O. A.; Megraw, T.; Zhang, F.; Brüschweiler, R. *ACS Chem. Biol.* **2015**, *10*, 452−459.
(8) Wishart, D. S.; Jewison, T.; Guo, A. C.; Wilson, M.; Knox, C.; Liu, Y.; Djoumbou, Y.; Mandal, R.; Aziat, F.; Dong, E.; Bouatra, S.; Sinelnikov, I.; Arndt, D.; Xia, J.; Liu, P.; Yallou, F.; Bjorndahl, T.; Perez-Pineiro, R.; Eisner, R.; Allen, F.; Neveu, V.; Greiner, R.; Scalbert, A. *Nucleic Acids Res.* **2012**, *41*, D801−D807.
(9) Vu, T. N.; L, K. *Metabolites* **2013**, *3*, 259−276.
(10) Emwas, A.-H. M.The Strengths and Weaknesses of NMR Spectroscopy and Mass Spectrometry with Particular Focus on Metabolomics Research. In *Metabonomics: Methods and Protocols*; Bjerrum, J. T., Ed.; Springer New York: New York, NY, 2015; pp 161−193.
(11) Tredwell, G. D.; Bundy, J.; De Iorio, M.; Ebbels, T. *Metabolomics* **2016**, *12*, 1−10.
(12) Lane, A. N.; Fan, T. W. M. *Arch. Biochem. Biophys.* **2017**, *628*, 123−131.
(13) Lane, A. N.; Higashi, R. M.; Fan, T. W. *TrAC, Trends Anal. Chem.* **2019**, *120*, No. 115322.
(14) Lin, P.; Lane, A. N.; Fan, T. W. *Methods Mol. Biol.* **2019**, *2037*, 151−168.
(15) Bax, A.; Subramanian, S. *J. Magn. Reson.* **1986**, *67*, 565−569.
(16) Robinette, S. L.; Brüschweiler, R.; Schroeder, F. C.; Edison, A. S. *Acc. Chem. Res.* **2012**, *45*, 288−297.
(17) Markley, J. L.; Ulrich, E. L.; Berman, H. M.; Henrick, K.; Nakamura, H.; Akutsu, H. *J. Biomol. NMR* **2008**, *40*, 153−155.
(18) Bingol, K.; Bruschweiler-Li, L.; Li, D.; Zhang, B.; Xie, M.; Brüschweiler, R. *Bioanalysis* **2016**, *8*, 557−573.
(19) Xia, J.; Bjorndahl, T. C.; Tang, P.; Wishart, D. S. *BMC Bioinf.* **2008**, *9*, 507.
(20) Kikuchi, J.; Tsuboi, Y.; Komatsu, K.; Gomi, M.; Chikayama, E.; Date, Y. *Anal. Chem.* **2016**, *88*, 659−665.
(21) Summers, M. F.; Marzilli, L. G.; Bax, A. *J. Am. Chem. Soc.* **1986**, *108*, 4285−4294.
(22) Kövér, K. E.; Hruby, V. J.; Uhrin, D. *J. Magn. Reson.* **1997**, *129*, 125−129.
(23) Zhang, F.; Brüschweiler, R. *Angew. Chem., Int. Ed.* **2007**, *46*, 2639−2642.
(24) Martin, G. E.; Hilton, B. D.; Blinov, K. A. *J. Nat. Prod.* **2011**, *74*, 2400−2407.
(25) Ulrich, E. L.; Akutsu, H.; Doreleijers, J. F.; Harano, Y.; Ioannidis, Y. E.; Lin, J.; Livny, M.; Mading, S.; Maziuk, D.; Miller, Z.; Nakatani, E.; Schulte, C. F.; Tolmie, D. E.; Kent Wenger, R.; Yao, H.; Markley, J. L. *Nucleic Acids Res.* **2007**, *36*, D402−D408.
(26) Bingol, K.; Zhang, F.; Bruschweiler-Li, L.; Brüschweiler, R. *Anal. Chem.* **2012**, *84*, 9395−9401.
(27) Wishart, D. S.; Feunang, Y. D.; Marcu, A.; Guo, A. C.; Liang, K.; Vazquez-Fresno, R.; Sajed, T.; Johnson, D.; Li, C.; Karu, N.; Sayeeda, Z.; Lo, E.; Assempour, N.; Berjanskii, M.; Singhal, S.; Arndt, D.; Liang, Y.; Badran, H.; Grant, J.; Serra-Cayuela, A.; Liu, Y.; Mandal, R.; Neveu, V.; Pon, A.; Knox, C.; Wilson, M.; Manach, C.; Scalbert, A. *Nucleic Acids Res.* **2018**, *46*, D608−D617.
(28) Delaglio, F.; Grzesiek, S.; Vuister, G. W.; Zhu, G.; Pfeifer, J.; Bax, A. *J. Biomol. NMR* **1995**, *6*, 277−293.
(29) Worley, B.; Powers, R. *J. Magn. Reson.* **2015**, *261*, 19−26.
(30) Worley, B.; Powers, R. *J. Magn. Reson.* **2015**, *261*, 19−26.
(31) Luan, T.; Jaravine, V.; Yee, A.; Arrowsmith, C. H.; Orekhov, V. Y. *J. Biomol. NMR* **2005**, *33*, 1−14.
(32) Nakabayashi, R.; Sawada, Y.; Yamada, Y.; Suzuki, M.; Hirai, M. Y.; Sakurai, T.; Saito, K. *Anal. Chem.* **2013**, *85*, 1310−1315.
(33) Williamson, R. T.; Buevich, A. V.; Martin, G. E.; Parella, T. *J. Org. Chem.* **2014**, *79*, 3887−3894.
(34) Furihata, K.; Seto, H. *Tetrahedron Lett.* **1995**, *36*, 2817−2820.
(35) Furrer, J. *Concept Magn. Reson., Part A* **2012**, *40*, 146−169.
(36) Schanda, P.; Brutscher, B. *J. Am. Chem. Soc.* **2005**, *127*, 8014−8015.
(37) Schoefberger, W.; Smrečki, V.; Vikić-Topić, D.; Müller, N. *Magn. Reson. Chem.* **2007**, *45*, 583−589.
(38) Clendinen, C. S.; Pasquel, C.; Ajredini, R.; Edison, A. S. *Anal. Chem.* **2015**, *87*, 5698−5706.
(39) Estrada, E. *Comput. Chem.* **2000**, *24*, 193−201.
(40) Miyashita, Y.; Okuyama, T.; Ohsako, H.; Sasaki, S. *J. Am. Chem. Soc.* **1989**, *111*, 3469−3470.
(41) Zhang, F.; Bruschweiler-Li, L.; Brüschweiler, R. *J. Am. Chem. Soc.* **2010**, *132*, 16922−16927.
(42) Kupče, Ē.; Claridge, T. D. W. *Angew. Chem., Int. Ed.* **2017**, *56*, 11779−11783.

https://doi.org/10.1021/acs.analchem.2c02902
Anal. Chem. 2022, 94, 16308−16318